A quantum molecular dynamics study of aqueous solvation dynamics

Pablo E. Videla, Peter J. Rossky, and D. Laria

Citation: The Journal of Chemical Physics **139**, 164506 (2013); doi: 10.1063/1.4826347
View online: http://dx.doi.org/10.1063/1.4826347
View Table of Contents: http://scitation.aip.org/content/aip/journal/jcp/139/16?ver=pdfcov
Published by the AIP Publishing

A quantum molecular dynamics study of aqueous solvation dynamics

Pablo E. Videla,[1] Peter J. Rossky,[2] and D. Laria[1,3,a)]
[1]*Departamento de Química Inorgánica Analítica y Química-Física e INQUIMAE, Facultad de Ciencias Exactas y Naturales, Universidad de Buenos Aires, Ciudad Universitaria, Pabellón II, 1428 Buenos Aires, Argentina*
[2]*Department of Chemistry and Biochemistry, The University of Texas at Austin, Austin, Texas 78712-0165, USA*
[3]*Departamento de Física de la Materia Condensada, Comisión Nacional de Energía Atómica, Avenida Libertador 8250, 1429 Buenos Aires, Argentina*

(Received 26 June 2013; accepted 8 October 2013; published online 23 October 2013)

Ring polymer molecular dynamics experiments have been carried out to examine effects derived from nuclear quantum fluctuations at ambient conditions on equilibrium and non-equilibrium dynamical characteristics of charge solvation by a popular simple, rigid, water model, SPC/E , and for a more recent, and flexible, q-TIP4P/F model, to examine the generality of conclusions. In particular, we have recorded the relaxation of the solvent energy gap following instantaneous, $\pm e$ charge jumps in an initially uncharged Lennard-Jones-like solute. In both charge cases, quantum effects are reflected in sharper decays at the initial stages of the relaxation, which produce up to a ∼20% reduction in the characteristic timescales describing the solvation processes. For anionic solvation, the magnitude of polarization fluctuations controlling the extent of the water proton localization in the first solvation shell is somewhat more marked than for cations, bringing the quantum solvation process closer to the classical case. Effects on the solvation response from the explicit incorporation of flexibility in the water Hamiltonian are also examined. Predictions from linear response theories for the overall relaxation profile and for the corresponding characteristic timescales are reasonably accurate for the solvation of cations, whereas we find that they are much less satisfactory for the anionic case. © *2013 AIP Publishing LLC*. [http://dx.doi.org/10.1063/1.4826347]

I. INTRODUCTION

Hydrogen bonding (HB) plays a key role as a controlling agent for practically all equilibrium and dynamical characteristics that make water a singular substance in nature. Solvation dynamics – i.e., the time dependent response of water following a modification of the electronic structure of a probe – is no exception. A large body of results extracted from direct experiments[1–5] and theoretical work[6–15] have clearly demonstrated that the ultrafast initial relaxation exhibited by liquid water is predominantly associated with small librational motions, involving subtle modifications of the overall architecture of hydrogen bonds in the close vicinity of the perturbed, typically excited state, solute.

In recent years, the analysis of the effects derived from the explicit incorporation of nuclear quantum fluctuations in computer simulations of liquid water has attracted considerable attention. In many cases, the dynamical analysis has been carried out from a path-integral perspective, via the implementation of approximate dynamical approaches, such as centroid molecular dynamics[16–22] or ring-polymer molecular dynamics[23–27] (RPMD) schemes, to cite two leading examples. By now, it is well established that zero-point energy and tunneling effects promote a global weakening in the strength of HB.[28,29] From the dynamical side, these effects are translated into sensible reductions of the characteristic timescales describing both translational and orientational motions.[23,25] Yet, the actual magnitude of these dynamical effects seems to be very much dependent on the particular choice of the force field adopted. For example, Habershon *et al.*[25] have thoroughly examined the q-TIP4P/F case, a model Hamiltonian that has been specifically designed to be implemented in path integral-based simulation experiments on pure water. In fact, their results revealed that the modifications in the diffusive characteristics of water, introduced from quantum fluctuations in the nuclei, were much less marked than those previously reported.[23] These smaller effects would be the result of a competition between the destabilization of HB, on average, counterbalanced by an increment in the water polarizability.

Within this general framework, in the present paper, we present RPMD results that aim at assessing the magnitude of nuclear quantum effects on the dynamical characteristics of aqueous solvation. As we mentioned above, a sizeable fraction of the overall solvation response of liquid water is clearly dominated by contributions from molecules lying in shells close to the solute species. Moreover, dynamical modes in these hydration layers are known to exhibit characteristic behaviors[30–34] which, in turn, would open the possibility for distinctive quantum effects on relaxation channels that are different from the homogeneous neat solvent.

Our analysis here will focus attention on the relaxation of the solvation structure in a classic model reaction, namely, the sudden modification of the charge on an, initially uncharged spherical solute. Given the charge asymmetric character of ionic solvation in water, we analyze both the cationic and

a)Author to whom correspondence should be addressed. Electronic mail: dhlaria@cnea.gov.ar

the anionic solvation cases. The gross features of our results confirm that nuclear quantum effects induce faster overall relaxation. Moreover, our observation suggests that the microscopic origins of these modifications can be ascribed not only to changes evident in the dynamics of the bulk liquid, but also to the distinct nature of the quantum polarization fluctuations induced locally by the solute species.

The organization of the present paper is as follows: Computational details are described in Sec. II. Our results are presented in Sec. III. Finally, in Sec. IV, the main conclusions of the work will be briefly summarized.

II. MODEL AND SIMULATION PROCEDURE

The systems under investigation were composed of a spherical solute particle (S) and $N_w = 215$ water (W) molecules, confined within a periodically replicated, cubic box of length $L = 18.6$ Å, thus having the number density of ambient liquid water. Effects on aqueous solvation from nuclear quantum fluctuations were evaluated using the RPMD scheme developed by Manolopoulos and co-workers.[27] The starting point of the methodology is the consideration of $Q_P(N, V, T)$, i.e., the P-bead, discretized imaginary time path integral representation of the canonical partition function for an N particle system at a temperature T, confined within a volume V,

$$Q_P = \frac{1}{h^{3PN}} \int \cdots \int \prod_{k=1}^{P} \prod_{i=1}^{N} \mathrm{d}\mathbf{r}_i^{(k)}\, \mathrm{d}\mathbf{p}_i^{(k)} e^{-\beta_P H_P(\{\mathbf{p}_i^{(k)}\},\{\mathbf{r}_i^{(k)}\})}. \tag{1}$$

In the equation given below, the Hamiltonian $H_P(\{\mathbf{p}_i^{(k)}\}, \{\mathbf{r}_i^{(k)}\})$ is defined as

$$\begin{aligned} H_P\left(\{\mathbf{p}_i^{(P)}\}, \{\mathbf{r}_i^{(P)}\}\right) &= \sum_{i=1}^{N} \sum_{k=1}^{P} \left[\frac{\left(\mathbf{p}_i^{(k)}\right)^2}{2M_i} + \frac{M_i}{2(\beta_P \hbar)^2} \left(\mathbf{r}_i^{(k)} - \mathbf{r}_i^{(k+1)}\right)^2 \right] \\ &\quad + \sum_{k=1}^{P} V\left(\mathbf{r}_1^{(k)}, \mathbf{r}_2^{(k)}, \ldots, \mathbf{r}_N^{(k)}\right), \end{aligned} \tag{2}$$

where $\beta_P = (P k_B T)^{-1}$ and $\mathbf{r}_i^{(k)}$ and $\mathbf{p}_i^{(k)}$ denote the position and momentum of the ith particle of mass M_i at the imaginary time slice k, respectively ($\mathbf{r}_i^{(P+1)} = \mathbf{r}_i^{(1)}$). Finally, the time evolution of the system in RPMD is provided by ansatz, as the classical Hamilton's equations of motion applied on $H_P(\{\mathbf{p}_i^{(P)}\}, \{\mathbf{r}_i^{(P)}\})$.

In our particular case, the potential energy term $V(\{\mathbf{r}\})$ in Eq. (2) included water-water and solute-water contributions, namely,

$$V(\{\mathbf{r}\}) = V_{ww}(\{\mathbf{r}\}) + V_{sw}(\{\mathbf{r}\}). \tag{3}$$

For $V_{ww}(\{\mathbf{r}\})$, we primarily adopted the SPC/E model.[35] We chose this simplified model for two reasons: first, the classical solvation dynamics in rigid polar fluids has been extensively analyzed in numerous studies;[6,11,12,36–38] moreover, quantum mechanical effects on translational and rotational motions of SPC/E water have also been examined, using a similar procedure to the one implemented in this work.[23] We have also explored the generality of conclusions obtained for SPC/E by considering a different and much newer model which also includes intramolecular flexibility in a reasonably realistic manner, the q -TIP4P/F Hamiltonian.[25] We carry out additional simulation experiments for solvation dynamics in this case as well, and compare the two models.

In all cases, solute-solvent interactions were modeled assuming pairwise, site-site, interactions of the Lennard-Jones plus Coulomb type:

$$V_{sw} = \sum_{i}^{N_w} \sum_{\alpha} u_{s\alpha}(|\mathbf{r}_s - \mathbf{r}_\alpha^i|) \tag{4}$$

with

$$u_{s\alpha}(r) = 4\epsilon_{s\alpha} \left[\left(\frac{\sigma_{s\alpha}}{r}\right)^{12} - \left(\frac{\sigma_{s\alpha}}{r}\right)^{6} \right] + \frac{z_s z_\alpha^w e^2}{r}, \tag{5}$$

where $\mathbf{r}_s$ and z_s denote the coordinate and partial charge of the solute and $\mathbf{r}_\alpha^i$ and z_α^w represent the position and partial charge of the α-site (α = O, H, H) in the ith water molecule ($i = 1, \ldots, N_w$). Following previous analysis,[37] we set $\sigma_s = 3.1$ Å, $\epsilon_s = 0.174$ kcal mole^{-1} and $M_s = 2.6 \times 10^{-23}$ g. For cross interactions, we adopted the usual arithmetic and geometric means for length and energy parameters, respectively.

Solvation was analyzed by performing two sets of simulation experiments: Equilibrium ensemble averages were collected from a series of 500 ps runs, corresponding to the canonical ensemble, controlled by an Andersen thermostat[39] set at $T = 298$ K. On the other hand, dynamical information was obtained from microcanonical runs at an ensemble of initial conditions. To integrate the equations of motion, we used two different time steps:[40] $\Delta t = 0.5$ fs to integrate the intermolecular interactions and $\delta t = \Delta t/4$ to integrate intramolecular coordinates in the q-TIP4P/F water molecules and harmonic terms in the polymer rings. To handle the long range nature of Coulomb interactions, we implemented Ewald sum techniques, via a particle mesh algorithm.[41] For systems with a net charge, we assumed the presence of a continuum neutralizing background. Constraints imposed on intramolecular distances in the SPC/E water molecules were handled with the SHAKE algorithm.[42,43] The number of polymer beads was set to $P = 6$ ($P = 32$) for the SPC/E (q-TIP4P/F) water models.[23,25]

Quantum nuclear fluctuations were not explicitly included in the – presumed relatively massive – solute particle; as such, P was fixed at 1 for the corresponding degrees of freedom, while the RPMD solute mass, M_s^{RPMD} was scaled by the particular P factor adopted for the W particles, i.e., $M_s^{\mathrm{RPMD}} = P \times M_s$.

III. RESULTS

A. Equilibrium solvation structures for spherical solutes

To begin our analysis, it will be instructive to briefly examine quantum effects on the solvation structures around spherical solutes. Fig. 1 contains classical and RPMD results for solute-solvent pair correlations functions of the

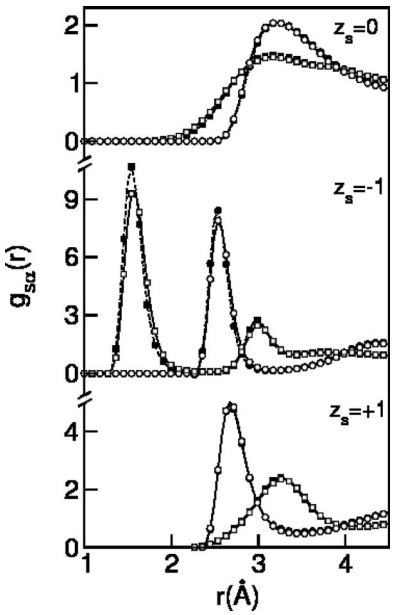

FIG. 1. Solute-oxygen (circles) and solute-hydrogen (squares) radial distribution functions for different spherical probes, dissolved in SPC/E water. RPMD and classical results are shown with open and filled symbols, respectively.

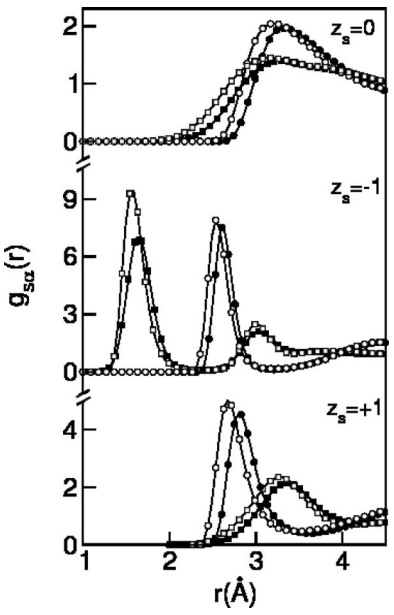

FIG. 2. Solute-oxygen and solute-hydrogen radial distribution functions for different spherical probes, dissolved in q-TIP4P/F (filled symbols) and SPC/E (open symbols). The site labeling is similar to the one shown in Fig. 1.

type

$$g_{s\alpha}(r) = \frac{L^3}{4\pi r^2 N_w} \sum_{i=1}^{N_w} \left\langle \delta\left(\left|\mathbf{r}_s - \mathbf{r}_\alpha^i\right| - r\right)\right\rangle_P \qquad (6)$$

for three different solute charges. In the previous equation, $\langle \cdots \rangle_P$ denotes an equilibrium ensemble average.

Effects from the explicit incorporation of quantum fluctuations in the SPC/E water nuclei are barely perceptible in the plots for $z_s = 0$ and for $z_s = +1$. For example, in the former case, the left side of the quantum g_{sH} at $r \sim 2.5$ Å appears slightly shifted towards the origin, whereas the magnitude of the first peak at $r = 3.1$ Å is a bit smaller than the one obtained for the classical case. Still, these differences are not translated into physically significant modifications either in the arrangement of the solvent or in the populations of solvation shells closest to the solute. However, the changes are more evident as one examines the solvation of anions. The modifications in the plots of $g_{\mathrm{s^-H}}$ and $g_{\mathrm{s^-O}}$ are manifested in a reduction in the magnitudes of the main peaks which, in turn, are also broadened and shifted towards larger values of r. Note that the latter features correlate, at a qualitative level, with the changes previously reported for site-site pair correlations in the neat solvent.[25,28] As such, the overall picture here would suggest that quantum effects on the spatial site-site correlations are not significant, on average, for pairs of particles whose intermolecular connectivity is not transferred via a H-bond, since the proton dispersion does not directly influence their interactions.

Before closing this section, it is also instructive to compare the characteristics of the solute-solvent density fields predicted by the two water model Hamiltonians investigated in this paper. We wish to emphasize that the comparisons in this paper are between Hamiltonian models which differ significantly in key structural and electrostatic parameters controlling the magnitude of the polarization fluctuations. This precludes a direct attribution of differences in results to specific elements of the potentials, such as flexibility. This will be evident from the density fields alone. In Fig. 2, we present results for different $g_{s\alpha}(r)$ for the three solutes in SPC/E and in q-TIP4P/F water, including the quantum treatment of the nuclei. As a general trend, note that, compared to the rigid SPC/E model results, the q-TIP4P/F peaks are somewhat broadened and slightly shifted, typically ~0.1 Å, towards longer distances. The physical interpretation of these differences is not straightforward. In fact, at first glance, some of them might even appear "unexpected." For example, one might predict that flexibility should produce a polarization of bonds in the water molecules lying in the first solvation shell of the anions, leading to an elongation of the O–H distance, and bringing the water protons closer to the charged solute. That is clearly not the result observed. In fact, it is of rather limited usefulness to increment a model used in a polar liquid with individual effects and use the observation to generalize the impact of such an effect, since, as demonstrated here, such effects interact and need to be incorporated in a self-consistent manner within a complete model. Hence, we largely refrain from making such attributions in our analysis.

B. Dynamical characteristics of solvation

The next step of our analysis will be the consideration of the solvation response of SPC/E water following a charge jump in an initially uncharged, spherical solute, such as might follow from a deprotonation or electron detachment. The model reactions that will be examined involve the following

ionization processes:

$$S \rightarrow S^{-}, \tag{7a}$$

$$S \rightarrow S^{+}; \tag{7b}$$

hereafter referred to as processes of type $\mathcal{A}$ and of type $\mathcal{C}$, respectively.

The usual route to monitor the solvent response involves the computation of $S(t)$, the non-equilibrium time correlation functions[44] defined as

$$S(t) = \frac{\left\langle E^{c}_{sw}(t) - E^{c}_{sw}(\infty)\right\rangle_{ne}}{\left\langle E^{c}_{sw}(0) - E^{c}_{sw}(\infty)\right\rangle_{ne}}. \tag{8}$$

$E^{c}_{sw}(t)$ represents the instantaneous Coulomb energy gap,

$$E^{c}_{sw}(t) = \Delta q V^{s}(t), \tag{9}$$

whereas Δq and $V^{s}(t)$ denote the charge jump and the instantaneous solvent electrostatic potential at the solute charge position. In Eq. (8), $\langle \cdots \rangle_{ne}$ represent a non-equilibrium ensemble average that was obtained from 100 RPMD-trajectories, whose initial conditions were taken from a canonical equilibrium run for a system containing an uncharged solute, at 5 ps time intervals. From these initial conditions, we modified the charge of the solute site by Δq, and monitored the relaxation of relevant observables along typical periods of about 2 ps.

Figure 3 contains results for the non-equilibrium RPMD-relaxations for processes $\mathcal{A}$ and $\mathcal{C}$. In addition, we have also included plots for the corresponding classical, i.e., $P = 1$, results. For $\Delta q = -e$ (top panel), the characteristics of the classical curve coincide with those reported in previous studies.[37] The relaxation exhibits a bimodal character: approximately one half of the total energy gap relaxes in an initial, ultrafast, decay with oscillatory characteristics that damp out after ~0.1 ps. During this time interval, the relaxation operates via librations restrained by H-bonds to nearby water molecules. This process is followed by a slower, diffusive stage, characterized by a time scale of the order of ~1 ps, during which the local densities of the different species reorganize toward the limiting spatial distributions shown in the central panel of Fig. 1.

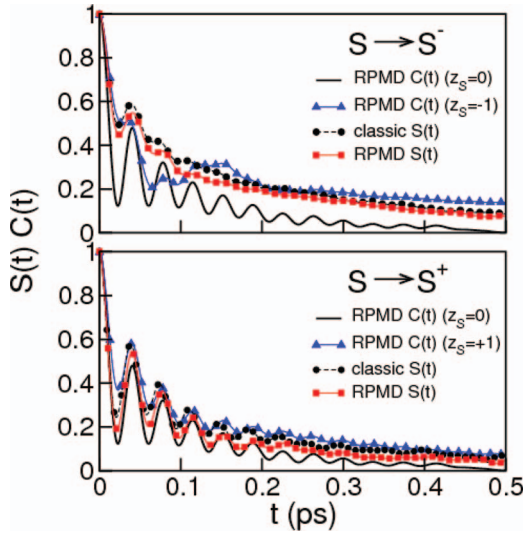

FIG. 3. Solvation responses of SPC/E water for the processes shown in Eqs. (7a) (top panel) and (7b) (bottom panel). Also shown are results from RPMD for the equilibrium energy gap autocorrelation function (Eq. (13)), $C(t)$, computed along equilibrium trajectories with uncharged and charged solutes.

TABLE I. Characteristic time scales for solvation.[a]

	τ_{slv}(ps)				
	SPC/E		q − TIP4P/F		
Process	Classical	RPMD	RPMD	$\tau^{cl}_{slv}/\tau^{qnt}_{slv}$	$\tau^{q-TIP}_{slv}/\tau^{SPC}_{slv}$
$\mathcal{A}$	0.15	0.13(0.22[b])	0.15(0.13[b])	1.15	1.15
$\mathcal{C}$	0.10	0.08(0.12[c])	0.12(0.15[c])	1.25	1.5
		0.06[d]	0.09[d]		1.5[d]

[a]From time integral of $S(t)$ up to 0.5 ps; after that time a single exponential decay was assumed, except as noted.
[b]From time integral of $C(t)$ ($z_s = -1$).
[c]From time integral of $C(t)$ ($z_s = +1$).
[d]From time integral of $C(t)$ ($z_s = 0$).

The explicit incorporation of quantum fluctuations in the water nuclei is manifested in the following modifications: (i) the initial decay looks somewhat larger (classical and RPMD results differ by ~10%); (ii) a more careful inspection also reveals a small shift towards lower frequencies in the initial librational motions; and (iii) an overall ~15% reduction in τ_{slv}, the characteristic solvation timescale, defined in terms of the time integral:

$$\tau_{slv} = \int_0^\infty S(t)\mathrm{d}t; \tag{10}$$

see entries in the fifth column of Table I. After 0.2 ps, classical and RPMD curves look practically identical, a fact consistent with the interpretation that the diffusive modes involved in the solvation relaxation are not affected by the explicit quantum treatment of the nuclei.

At a qualitative level, the overall characteristics of classical and RPMD relaxations for type $\mathcal{C}$ processes do not differ substantially from the previous, anionic, description. The initial RPMD decay looks more rapid, the damping is noticeably weaker and the fraction of the total relaxation associated with diffusive motions is markedly reduced. The combined effects of these modifications leads to a ~25% reduction in the overall solvation timescale (see entries in the fifth column of Table I).

In this case though, the underdamped character of the initial decays allows a more clear identification of the frequency reduction of the initial oscillations, from the inspections of the Fourier decompositions of the different relaxations, namely,

$$\hat{S}(\omega) = \int_0^\infty S(t)\ \cos(\omega t)\ \mathrm{d}t. \tag{11}$$

Plots of $\hat{S}(\omega)$ within the frequency domain of the rotation/libration band of water are shown in Fig. 4. Although some of the signals are still somewhat noisy, one can observe that the high frequency shoulders of the two RPMD curves at $\omega \sim 900$ cm^{-1} (shown with open symbols) appear shifted towards smaller frequencies, compared to the classical plots (shown with black symbols).

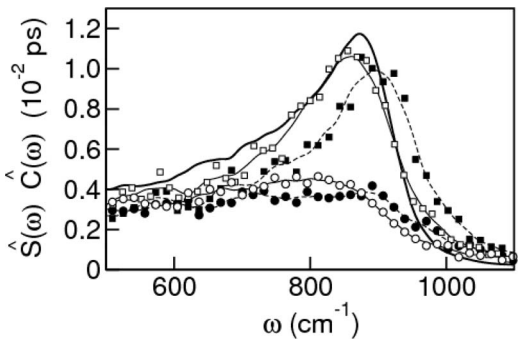

FIG. 4. Fourier transform of the non-equilibrium solvation relaxations for processes $\mathcal{A}$ (circles) and $\mathcal{C}$ (squares) in SPC/E water. The open (filled) symbols correspond to RPMD (classical), $\hat{S}(\omega)$, results. The thick solid line corresponds to RPMD $\hat{C}(\omega)$ evaluated with $z_s = 0$.

Interestingly, the origins of some of the differences presented in the two previous examples can be traced back to related effects observed in pure SPC/E water. In particular, the reductions of the overall solvation timescales seem to go hand-in-hand with the ones registered for the timescale characterizing orientational relaxations in the pure liquid,[23] although, in the latter case, the changes are somewhat larger (of the order of ∼35%). Similar arguments can be invoked to explain the shifts in the Fourier spectra shown in Fig. 4, which have also been reported in the decompositions of the orientational correlations of SPC/E water. In both cases, the causes of these modifications has been ascribed to a weakening of the strength of the W-W HB due to zero-point energy and tunneling effects.

One still may wonder why quantum effects appear somewhat more vividly for the relaxation of type $\mathcal{C}$ compared to that of type $\mathcal{A}$. Looking for clues to rationalize these differences, we focus attention on the overall structures of the ring-polymers associated with H-sites. In particular, we computed correlation, or quantum dispersion, lengths, $\mathcal{R}$, from the mean square displacements evaluated at the imaginary time slice $P/2$, namely,[45]

$$\mathcal{R}^2 = \frac{1}{P}\sum_{j=1}^{P}\left\langle\left|\mathbf{r}_{\mathrm{H}}^{(j+P/2)} - \mathbf{r}_{\mathrm{H}}^{(j)}\right|^2\right\rangle_P. \tag{12}$$

The length scale $\mathcal{R}$ gauges the extent of the spatial delocalization of the quantum particles and spans from the free, i.e., non-interacting, result – which is close to the thermal wavelength of the proton, $\lambda_{pr} \sim 0.4$ Å – down to smaller values, which depend on the characteristics of the confinement imposed by the coupling with the particular environment considered. For the classical particles, $\mathcal{R}^2$ vanishes. In the present case, the key element controlling the resulting value of $\mathcal{R}$ will be the nature of the polarization fluctuations prevailing in the vicinity of the tagged particle.

We started by analyzing the H-sites that participate in $S^-\cdots H$–O bonds, which lie under the first peak of the S^--H pair correlation function (see middle plots in Fig. 1). For this particular set, we found $\mathcal{R} = 0.15$ Å. On the other hand, a similar analysis performed upon the H-sites located under the much broader peak of g_{S^+H} at $r \sim 3.2$ Å (see bottom plots in Fig. 1) yielded $\mathcal{R} = 0.22$ Å, a value that practically coincides with the one observed for H-sites in bulk SPC/E water.

Given the stronger nature of the ion-water Coulomb coupling compared to the typical energy involved in a W-W hydrogen bond, the latter observation could have been expected qualitatively. Invoking basic electrostatic arguments, the localization of the H-site charges in close contact with the anion is clearly beneficial from an energetic perspective and, consequently, may reduce quantum spatial dispersion, bringing the solvation structure closer to the one expected in a classical simulation experiment. Conversely, for processes of type $\mathcal{C}$, the dynamics involved in the accommodation of the architecture of hydrogen bonds between the first and second solvation shell of the cation would be important and more akin to those observed in spontaneous breaking-and-reconstructing processes of hydrogen bonds operating in the bulk.

Considering the ∼50% differences reported in the quantum treatment of the diffusion coefficient of bulk SPC/E water,[23] the absence of meaningful modifications in the diffusive tails of $S(t)$ would also appear like a somewhat puzzling observation. The simple analysis of the timescales involved in the diffusive elements of relaxation can provide some physical arguments to analyze this feature: Note that a crude estimate of such timescales could be obtained from the shift of about $\Delta\ell = \sim 0.5$ Å, between the positions of the main peaks of the solute-oxygen pair correlation functions for the initial $z_s = 0$ configurations and the $t \to \infty$, i.e., $z_s = \pm 1$, limiting cases (see Fig. 1). Typically, in the bulk, water molecules cover distances of this order of $\Delta\ell$ via inertial displacements, in a few tenths of a picosecond, a timescale which is much shorter than the typical lifetime of a hydrogen bond in SPC/E water. As a consequence, we suggest that the rearrangements in the spatial distributions will be connected with individual displacements, preferentially, as the particles become "dragged" by solute-solvent Coulomb coupling, with practically no contribution from collective modes that would be otherwise controlled, again, by the hydrogen-bond dynamics. Hence, the bulk diffusion and the tail of $S(t)$ need not respond similarly.

In Fig. 5, we present, for comparison, RPMD results for relaxation using the flexible q-TIP4P/F Hamiltonian. The

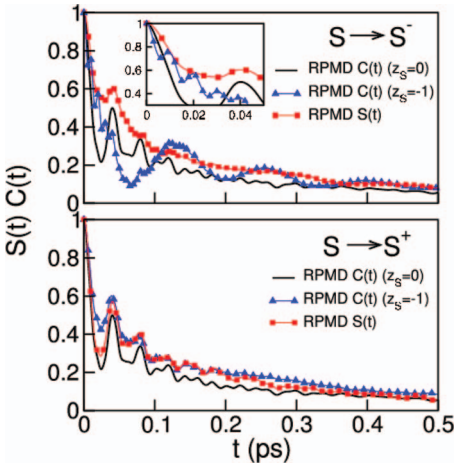

FIG. 5. Solvation responses of q-TIP4P/F water from RPMD. Otherwise, the same as Fig. 3.

qualitative trends for anionic and cationic solvation, reported above for SPC/E simulations, remain valid. Nevertheless, the entries in Table I reveal that the global solvation time scales for the q-TIP4P/F Hamiltonian manifest increments indicating that longer time spans are required for the reaccommodation of the larger number of degrees of freedom involved in the spatial and orientational relaxation for this model. Interestingly, some of these changes can be correlated with similar modifications operating in the orientational dynamics of the pure phases; for example, the quantum characteristic timescale for the dipole orientational relaxation of q-TIP4P/F water[25] is practically 1.6 times larger than the one reported for the rigid SPC/E model,[23] i.e., $\tau_{dip}^{\mathrm{q-TIP}} = 4.64$ ps versus $\tau_{dip}^{\mathrm{SPC}} = 2.94$ ps. Note that the latter ratio is of similar magnitude to the one found, in the present case, between $\tau_{slv}^{\mathrm{q-TIP}}$ and $\tau_{slv}^{\mathrm{SPC}}$ for the $\mathcal{C}$-type relaxation (see entries in the last column of Table I).

To complete our analysis, we examine the predictive capacity of linear theories in the present context. Following Onsager's regression hypothesis, and for sufficiently small perturbations, the nonequilibrium responses can be approximated by equilibrium time correlation functions, $C(t)$ of the type:[44]

$$S(t) \simeq C(t) = \frac{\left\langle \delta E_{sw}^{c}(t)\delta E_{sw}^{c}(0)\right\rangle_{P}}{\left\langle \left(\delta E_{sw}^{c}\right)^{2}\right\rangle_{P}}, \tag{13}$$

computed in the ensemble lacking the charge perturbation. In the previous equation, $\delta\mathcal{O} = \mathcal{O} - \langle\mathcal{O}\rangle_{P}$.

Results for RPMD-$C(t)$ have also been included in the two panels composing Figs. 3 and 5, the results being the same for $\mathcal{A}$ and $\mathcal{C}$ processes. Before attempting any comparison, the magnitude of the differences previously described in the relaxations for processes of type $\mathcal{A}$ and $\mathcal{C}$ already suggest that effects from nonlinearities in the solvation responses are likely to be non-negligible, at least in one of these cases. The nonlinearity is particularly evident in $\mathcal{A}$-type reactions; the entries in the last row of Table I show that the linear response prediction for τ_{slv} would correspond to a process twice as fast as the one recorded in the non-equilibrium relaxation experiments. Moreover, the amplitudes of the initial oscillations that modulate the $C(t)$ profile during the first 0.3 ps, are significantly reduced in the $S(t)$ relaxation and practically vanish beyond, say, ∼500 fs.

The quality of the agreement does not change substantially if one computes τ_{slv} from the correlation time for the spontaneous fluctuations of the solvent energy gap sampled along the ionized state potential energy surface. The plot of the corresponding $C(t)$ for $z_s = -1$ is also depicted in the top panel of Fig. 3 and its time integral is listed in Table I. Note that the latter curve follows the non-equilibrium $S(t)$ only during a ∼0.04 ps initial time interval, while it exhibits a much slower exponential decay at longer times. As a result, the equilibrium estimate for τ_{slv} is practically twice as large as the non-equilibrium value. A comparative analysis performed for the q-TIP4P/F model (see Fig. 5) shows similar characteristics, with the exception of a new feature in $C(t)$: there is a new ultrafast, ∼10 fs, mode, which can be ascribed to the proton stretching mode along the linear $S^{-}\cdots$H–O hydrogen bond (see inset in the top panel of Fig. 5). Note that this potential relaxation channel is not evident in $S(t)$, since it would be operative only after a time span longer than the one required for the above mentioned HB to be established via librational displacement, a time which is comparable to τ_{slv}. As such, even for this flexible Hamiltonian, the librational motions would still be the main controlling modes for the overall ionic solvation dynamics.

In contrast, the agreement for the SPC/E model is much more satisfactory for $\mathcal{C}$-type reactions. Not only is the difference between the τ_{slv} entries in Table I reduced to ∼25%, but also, and more importantly, the $C(t)$ plots in Figs. 3 and 5 reproduce the main features of the rotational and the diffusional stages of the corresponding non-equilibrium relaxations remarkably well. The distinctions between $\mathcal{A}$ and $\mathcal{C}$ processes can, again, be linked to the direct coupling of solvent and solute through a H-bond in $\mathcal{A}$ but not in $\mathcal{C}$. Correspondingly, there is a longer structural change in process $\mathcal{A}$, which also induces the librational dephasing evident in the relatively smoother $S(t)$ for process $\mathcal{A}$.

IV. CONCLUDING REMARKS

In this paper, we have examined effects derived from the explicit incorporation of quantum nuclear fluctuations on equilibrium and dynamical aspects pertaining to the solvation of a simple spherical solute in aqueous media at ambient conditions. An analysis based on the characteristics of site-site solute-solvent spatial correlations reveals that such effects provoke negligible modifications in the structure of the closest solvation shells of neutral and positively charged solutes. These modifications are more evident in the case of anions and are clearly manifested in the characteristics of the first peak of $g_{s\mathrm{H}}(r)$ which becomes broadened and shifted towards larger distances.

For the SPC/E model, nuclear quantum effects promote somewhat larger short-time decays at the inception of the relaxation processes, reflecting high frequency librational motions. Moreover, the subsequent oscillatory stages present slight reductions in the characteristic frequencies. These features are more evident in the case of the cationic solvation, due to the underdamped character of this intermediate dynamical regime. In spite of the ∼50% increment reported for the quantum impact on the diffusion coefficient of bulk SPC/E water,[23] the present simulation results show practically no modifications in the longer time tails of the solvation relaxation, which we attribute to local motions.

A global basis for comparison, established in terms of the corresponding time integrals of the relaxation, shows that quantum effects tend to hasten the response of the solvent, most likely due to the reduced rigidity of its hydrogen bond architecture. These dynamical modifications are somewhat more marked in the case of cationic species. The analysis of spatial delocalization of H-sites in the first hydration shell provides a physical argument to support this tendency. In particular, we found that the magnitude of the position dispersion for H-atoms in water molecules participating in $S^{-}\cdots$H–O bonds is ∼65% smaller than the one found for H-sites lying in the closest solvation shell of S^{+} species. This smaller dispersion, in turn, would reduce the impact of quantization on

solvation dynamics for S^- species, making it more similar to the one prevailing in simulations with a classical, i.e., point-position, description of the distribution of the solvent nuclei.

The explicitly flexible q-TIP4P/F model appears to somewhat slow the solvation dynamics. This retardation might be ascribed to the larger number of degrees of freedom involved in the overall relaxation processes. For $\mathcal{C}$-type relaxations, the changes in the characteristic solvation timescale correlate with similar modifications reported for the orientational dynamics in the bulk.[23] Within the present quantum perspective, we also analyzed the quality of linear theories for solvation dynamics. Our RPMD results show that the equilibrium time correlation function for the solvent energy gap yields a poor approximation for $\mathcal{A}$-type relaxations; in contrast, it reproduces the main features of the $\mathcal{C}$-type $S(t)$ curve remarkably well and provides an estimate for τ_{slv} which differs from the non-equilibrium value by only about ∼25%.

ACKNOWLEDGMENTS

D.L. is a staff member of CONICET (Argentina). P.J.R. acknowledges the support of this research by the U. S. National Science Foundation (NSF) (CHE-0910499). Additional support has been provided by the R. A. Welch Foundation (F-0019).

[1]P. F. Barbara and W. Jarzeba, Adv. Photochem. **15**, 1 (1990).
[2]M. Maroncelli, J. Mol. Liq. **57**, 1 (1993).
[3]R. Jimenez, G. R. Fleming, P. V. Kumar, and M. Maroncelli, Nature (London) **369**, 471 (1994).
[4]B. Zolotov, A. Gan, B. D. Fainberg, and F. D. Huppert, Chem. Phys. Lett. **265**, 418 (1997).
[5]M. J. Lang, X. J. Jordanides, X. Song, and G. R. Fleming, J. Chem. Phys. **110**, 5884 (1999).
[6]J. Bader and D. Chandler, Chem. Phys. Lett. **157**, 501 (1989).
[7]B. Bagchi, Annu. Rev. Phys. Chem. **40**, 115 (1989).
[8]P. V. Kumar and B. L. Tembe, J. Chem. Phys. **97**, 4356 (1992).
[9]M. Maroncelli, P. V. Kumar, and A. Papazyan, J. Phys. Chem. **97**, 13 (1993).
[10]P. J. Rossky and J. D. Simon, Nature (London) **370**, 263 (1994).
[11]B. J. Schwartz and P. J. Rossky, J. Phys. Chem. **101**, 6917 (1994).
[12]M. Re and D. Laria, J. Phys. Chem. B **101**, 10494 (1997).
[13]N. Nandi, K. Bhattacharyya, and B. Bagchi, Chem. Rev. **100**, 2013 (2000).
[14]C. Brooksby, O. V. Prezhdo, and P. J. Reid, J. Chem. Phys. **118**, 4563 (2003).
[15]B. Bagchi and B. Jana, Chem. Soc. Rev. **39**, 1936 (2010).
[16]F. Paesani, W. Zhang, D. A. Case, T. E. Cheatham, and G. A. Voth, J. Chem. Phys. **125**, 184507 (2006).
[17]T. D. Hone, P. J. Rossky, and G. A. Voth, J. Chem. Phys. **124**, 154103 (2006).
[18]F. Paesani, S. Iuchi, and G. A. Voth, J. Chem. Phys. **127**, 074506 (2007).
[19]A. Witt, S. D. Ivanov, M. Shiga, H. Forbert, and D. Marx, J. Chem. Phys. **130**, 194510 (2009).
[20]F. Paesani, S. S. Xantheas, and G. A. Voth, J. Phys. Chem. B **113**, 13118 (2009).
[21]F. Paesani and G. A. Voth, J. Chem. Phys. **132**, 014105 (2010).
[22]S. D. Ivanov, A. Witt, M. Shiga, and D. Marx, J. Chem. Phys. **132**, 031101 (2010).
[23]T. F. Miller III and D. E. Manolopoulos, J. Chem. Phys. **123**, 154504 (2005).
[24]S. Habershon, G. S. Fanourgakis, and D. E. Manolopoulos, J. Chem. Phys. **129**, 074501 (2008).
[25]S. Habershon, T. E. Markland, and D. E. Manolopoulos, J. Chem. Phys. **131**, 024501 (2009).
[26]S. Habershon and D. E. Manolopoulos, J. Chem. Phys. **131**, 244518 (2009).
[27]S. Habershon, D. E. Manolopoulos, T. E. Marklan, and T. F. Miller III, Annu. Rev. Phys. Chem. **64**, 387 (2013).
[28]R. A. Kuharski and P. J. Rossky, J. Chem. Phys. **82**, 5164 (1985).
[29]A. Wallqvist and B. J. Berne, Chem. Phys. Lett. **117**, 214 (1985).
[30]J. D. Smith, R. J. Saykally, and P. L. Geissler, J. Am. Chem. Soc. **129**, 13847 (2007).
[31]M. F. Kropman and H. J. Bakker, Science **291**, 2118 (2001).
[32]S. K. Pal, J. Peon, B. Bagchi, and A. H. Zewail, J. Phys. Chem. B **106**, 12376 (2002).
[33]D. Laage and J. T. Hynes, Proc. Natl. Acad. Sci. U.S.A. **104**, 11167 (2007).
[34]K. J. Tielrooij, S. T. van der Post, J. Hunger, M. Bomm, and H. J. Bakker, J. Phys. Chem. B **115**, 12638 (2011).
[35]H. J. C. Berendsen, J. R. Grigera, and T. P. Straatsma, J. Phys. Chem. **91**, 6269 (1987).
[36]M. Rao and B. J. Berne, J. Phys. Chem. **85**, 1498 (1981).
[37]M. Maroncelli and G. R. Fleming, J. Chem. Phys. **89**, 5044 (1988).
[38]B. D. Bursulaya, D. A. Zichi, and H. J. Kim, J. Phys. Chem. **99**, 10069 (1995).
[39]J. C. Andersen, J. Chem. Phys. **72**, 2384 (1980).
[40]M. Tuckerman, B. J. Berne, and G. J. Martyna, J. Chem. Phys. **97**, 1990 (1992).
[41]U. Essmann, L. Perera, M. L. Berkowitz, T. Darden, H. Lee, and L. G. Pedersen, J. Chem. Phys. **103**, 8577 (1995).
[42]J. P. Ryckaert, G. Ciccotti, and H. J. C. Berendsen, J. Comput. Phys. **23**, 327 (1977).
[43]G. Ciccotti and J. P. Ryckaert, Comp. Phys. Rep. **4**, 346 (1986).
[44]D. Chandler, *Introduction to Modern Statistical Mechanics* (Oxford University Press, New York, 1987), Chap. 8.
[45]A. L. Nichols, D. Chandler, Y. Singh, and D. M. Richardson, J. Chem. Phys. **81**, 5109 (1984).